

RESEARCH ARTICLE

# NUP98-PHF23 Is a Chromatin-Modifying Oncoprotein That Causes a Wide Array of Leukemias Sensitive to Inhibition of PHD Histone Reader Function

Sheryl M. Gough<sup>1</sup>, Fan Lee<sup>1</sup>, Fan Yang<sup>1</sup>, Robert L. Walker<sup>1</sup>,  
Yeulin J. Zhu<sup>1</sup>, Marbin Pineda<sup>1</sup>, Masahiro Onozawa<sup>1</sup>,  
Yang Jo Chung<sup>1</sup>, Sven Bilke<sup>1</sup>, Elise K. Wagner<sup>3</sup>,  
John M. Denu<sup>3</sup>, Yi Ning<sup>2</sup>, Bowen Xu<sup>4</sup>, Gang Greg Wang<sup>4</sup>,  
Paul S. Meltzer<sup>1</sup>, and Peter D. Aplan<sup>1</sup>

## ABSTRACT

In this report, we show that expression of a NUP98-PHF23 (NP23) fusion, associated with acute myeloid leukemia (AML) in humans, leads to myeloid, erythroid, T-cell, and B-cell leukemia in mice. The leukemic and preleukemic tissues display a stem cell-like expression signature, including *Hoxa*, *Hoxb*, and *Meis1* genes. The PHF23 plant homeodomain (PHD) motif is known to bind to H3K4me3 residues, and chromatin immunoprecipitation experiments demonstrated that the NP23 protein binds to chromatin at a specific subset of H3K4me3 sites, including at *Hoxa*, *Hoxb*, and *Meis1*. Treatment of NP23 cells with disulfiram, which inhibits the binding of PHD motifs to H3K4me3, rapidly and selectively killed NP23-expressing myeloblasts; cell death was preceded by decreased expression of *Hoxa*, *Hoxb*, and *Meis1*. Furthermore, AML driven by a related fusion gene, NUP98-JARID1A (NJL), was also sensitive to disulfiram. Thus, the NP23 mouse provides a platform to evaluate compounds that disrupt binding of oncogenic PHD proteins to H3K4me3.

**SIGNIFICANCE:** NP23 and NJL belong to a subset of chromatin-modifying fusion oncoproteins that cause leukemia characterized by overexpression of *Hoxa* and *Meis1* genes. Inhibition of NP23 binding to H3K4me3 at *Hoxa* and *Meis1* loci by disulfiram, a U.S. Food and Drug Administration-approved drug, leads to leukemic cell death, demonstrating the feasibility of targeting this subset of oncoproteins.

*Cancer Discov*; 4(5); 564–77. ©2014 AACR.

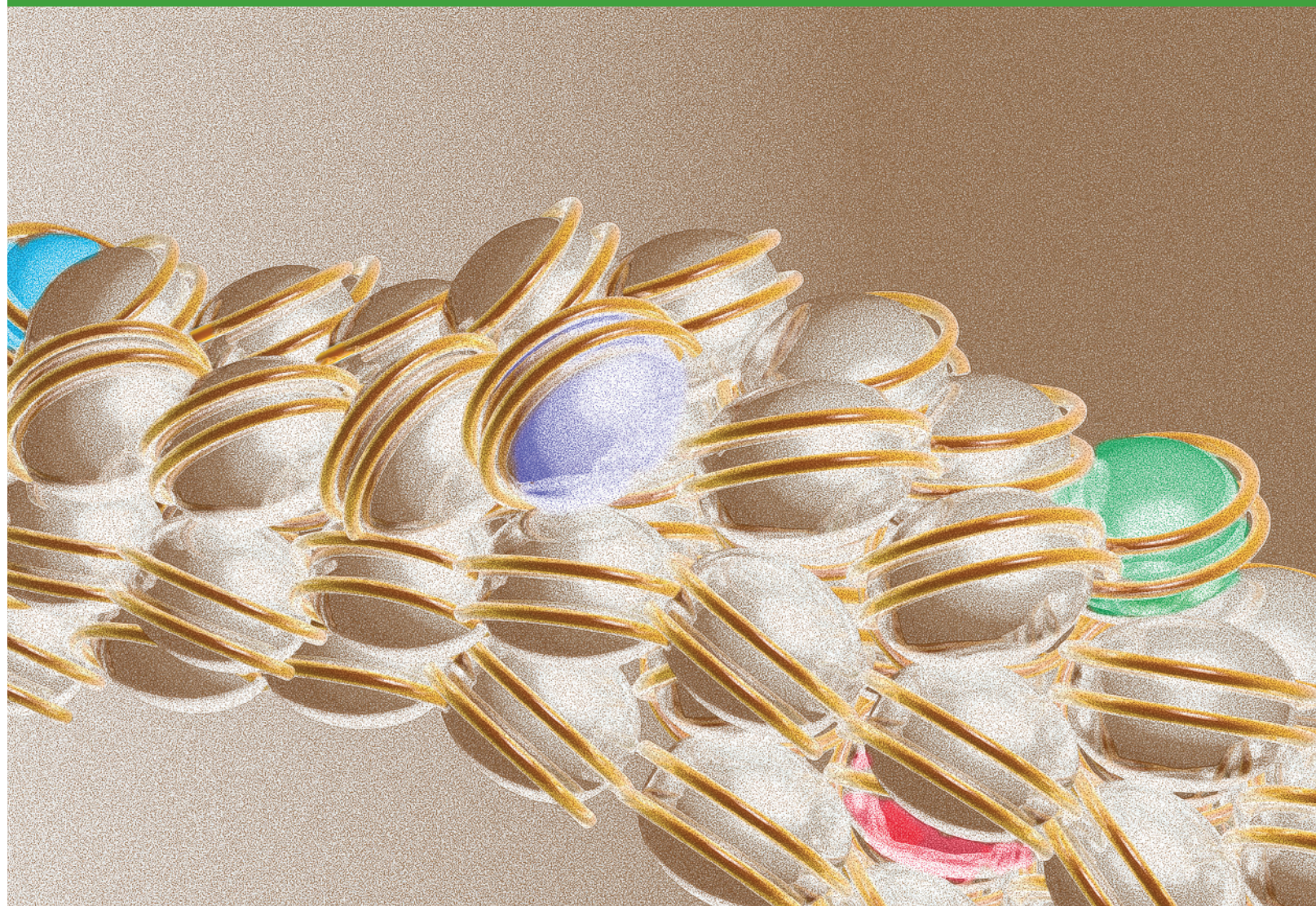
**Authors' Affiliations:** <sup>1</sup>Genetics Branch, Center for Cancer Research, National Cancer Institute, NIH, Bethesda; <sup>2</sup>Department of Pathology, Johns Hopkins University, Baltimore, Maryland; <sup>3</sup>Department of Biomolecular Chemistry, University of Wisconsin, Madison, Wisconsin; and <sup>4</sup>Lineberger Comprehensive Cancer Center, University of North Carolina at Chapel Hill School of Medicine, Chapel Hill, North Carolina

**Note:** Supplementary data for this article are available at *Cancer Discovery* Online (<http://cancerdiscovery.aacrjournals.org/>).

**Corresponding Author:** Peter D. Aplan, Genetics Branch, Center for Cancer Research, National Cancer Institute, NIH, Building 37, Room 6002, 37 Convent Drive, Bethesda, MD 20892. Phone: 301-435-5005; Fax: 301-496-0047; E-mail: [aplanp@mail.nih.gov](mailto:aplanp@mail.nih.gov)

**doi:** 10.1158/2159-8290.CD-13-0419

©2014 American Association for Cancer Research.



## INTRODUCTION

Nucleoporin 98-kDa (*NUP98*) gene fusions are associated with a wide range of hematologic malignancies, including *de novo* and therapy-related acute myeloid leukemia (AML), chronic myeloid leukemia in blast crisis (CML-bc), acute lymphoid leukemia (ALL), and myelodysplastic syndrome (MDS); at least 29 different *NUP98* partner genes have been identified (1, 2). Although *NUP98* fusions were initially considered to be infrequent events, the use of high-resolution technologies, such as FISH, array comparative genomic hybridization, and single-nucleotide polymorphism arrays, has led to the detection of cryptic rearrangements of *NUP98* with increasing frequency. In fact, a single *NUP98* gene fusion (*NUP98-NDS1*) was recently found in 16.1% of pediatric cytogenetic-normal AML and in 2.3% of adult cytogenetic-normal AML (3).

Many *NUP98* fusions have been shown to alter normal hematopoietic stem and progenitor cell (HSPC) gene expression programs, characterized by overexpression of *Hoxa7*, *Hoxa9*, and *Hoxa10* (1, 4, 5). Overexpression of *HOXA* genes, particularly *HOXA5*, *HOXA7*, *HOXA9*, and *HOXA10*, has been

identified in a large subset of AML, pre-B-ALL, and precursor T-cell lymphoblastic lymphoma/leukemia (pre-T LBL) patients and is associated with a poor prognosis (2, 3, 6–9). Regulation of *HOXA* gene expression is achieved in part via activating and silencing epigenetic processes, including histone modifications, at specific developmental stages. Abnormal expression caused by aberrant application (“writing”) or recognition (“reading”) of histone modifications is associated with malignant transformation in a number of settings (10, 11). Indeed, one of the best-studied examples of this phenomenon is the aberrant histone modification and resultant changes in *HOXA* gene expression in leukemias associated with *MLL* gene fusions (12, 13).

A recurrent t(11;17)(p15;p13) translocation in patients with AML leads to the production of a *NUP98-PHF23* (hereafter *NP23*) fusion gene, which encodes a chimeric protein that juxtaposes the amino-terminal portion of *NUP98* to the carboxy-terminal portion of plant homeodomain (PHD) finger 23 (*PHF23*; ref. 14 and Ning, unpublished data). The *PHF23* PHD motif is retained in the fusion and is similar to the *JARID1A* PHD motif, which is known to bind to H3K4me3 (15),

implicating the NP23 fusion as a putative aberrant chromatin modifier. In addition, the expression of NP23 in wild-type (WT) mouse bone marrow (BM) cells stimulates *Hoxa9* expression and myeloid progenitor cell proliferation *in vitro* (15).

To determine the spectrum of hematopoietic cell types that could be transformed by a *NP23* fusion, we generated transgenic mice that expressed the *NP23* fusion in hematopoietic tissues, using *Vav1* regulatory elements. We performed global gene expression assays and genome-wide chromatin immunoprecipitation (ChIP) followed by next-generation sequencing (ChIP-seq) to identify aberrant gene expression

signatures and chromatin modifications associated with the *NP23* fusion.

## RESULTS

### *In Vivo Expression of NP23 in Hematopoietic Cells Results in Decreased Survival and Leukemic Transformation*

We generated transgenic mice that expressed *NP23* in mouse hematopoietic tissues (Fig. 1A–C and Supplementary Fig. S1A), and studied progeny from two *NP23* founders (B10 and C10). Complete blood counts (CBC) were obtained every

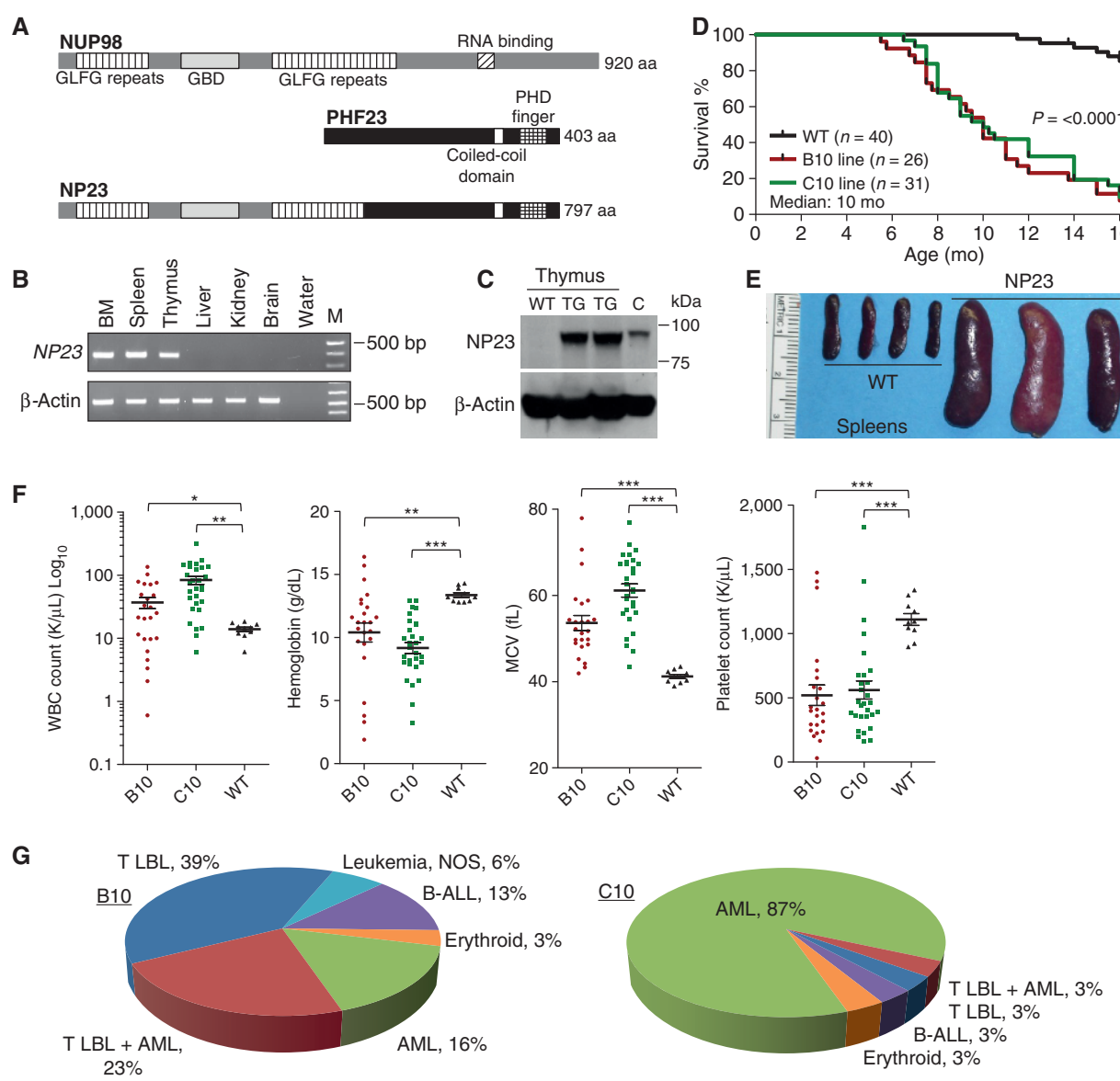


**Figure 1.** The NP23 fusion protein is a multilineage oncogene. **A**, NUP98 (top), PHF23 (middle), and the aberrant NP23 fusion protein (bottom). **B**, expression of the NP23 transgene in BM, spleen, and thymus. **C**, immunoblot of NP23 protein in NP23 transgenic (TG) thymus. C, positive control. **D**, survival curves of B10, C10, and WT littermate controls. **E**, representative necropsy images of splenomegaly in NP23-positive leukemia. **F**, WBC, Hgb, MCV, and platelet counts at disease presentation. Note the log<sub>10</sub> scale on WBC graph. **G**, frequency of leukemia subtypes by founder line. Some mice found dead with evidence of leukemia could not be further evaluated and are designated "leukemia, not otherwise specified (NOS)." The t test, \*, P < 0.05; \*\*, P < 0.01; \*\*\*, P < 0.001. WBC, white blood cell; MCV, mean corpuscular volume.

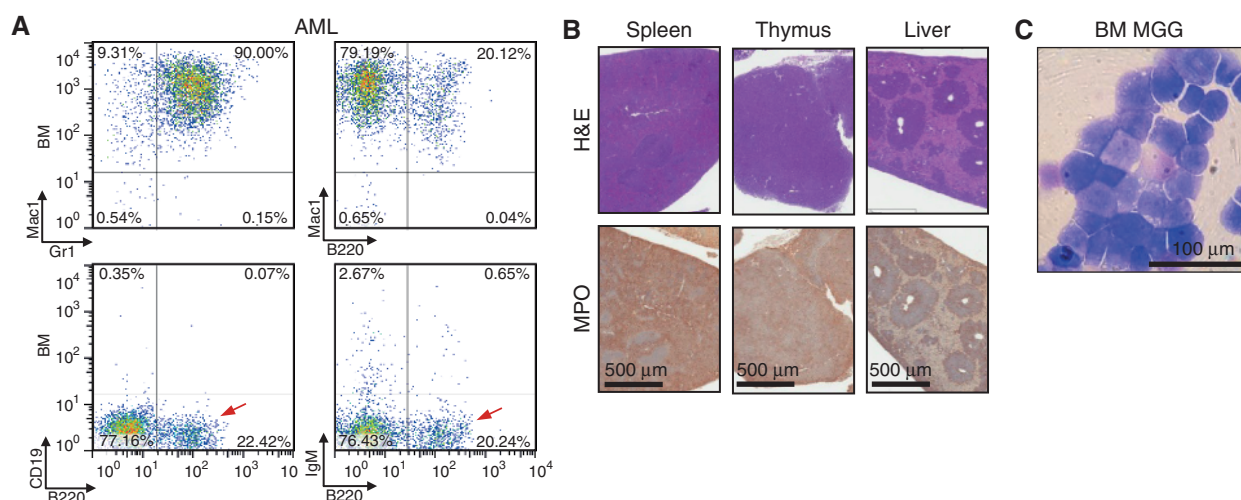


**Figure 2.** NP23 AML. **A**, AML from mouse 820; FACS profiles show Mac1<sup>+</sup>/Gr1<sup>+</sup> and Mac1<sup>+</sup>/B220<sup>dim</sup> cells in the BM. The B220<sup>+</sup> cells are CD19<sup>+</sup> and sIgM-negative (red arrows) and are therefore not typical B cells. **B**, H&E and MPO IHC of spleen, thymus, and liver showing loss of normal organ architecture and infiltration of MPO<sup>+</sup> malignant cells. **C**, May-Grünwald Giemsa (MGG) stained BM myeloblasts. FACS, fluorescence-activated cell sorting; MPO, myeloperoxidase.

2 months. Offspring of the B10 and C10 founders appeared healthy for the first 5 months of life, with only modestly altered CBCs. The NP23 mice showed a nonsignificant trend toward anemia, an increase in mean corpuscular volume (MCV), and no difference in the absolute neutrophil count compared with WT littermates (Supplementary Fig. S1B). Although no consistent differences were observed in the absolute lymphocyte count between the B10 line and WT mice, mice from the C10 line showed an absolute lymphopenia at 6 to 12 months of age.

The B10 and C10 transgenic mice showed markedly ( $P < 0.0001$ ) decreased survival compared with that of their WT littermates (Fig. 1D). Median survival of both B10 and C10 progeny was 10 months, and onset of disease was quite variable, ranging from 5 to 18 months of age. Signs of disease included weight loss, lethargy, kyphosis, dyspnea, visible lymphadenopathy, and abnormal CBCs. Necropsy of sick NP23 mice typically revealed hepatomegaly, splenomegaly (Fig. 1E), and lymphadenopathy; thymoma was present in most cases of pre-T LBL. At disease presentation, CBCs typically revealed elevated white blood cell (WBC) counts, macrocytic anemia, and thrombocytopenia (Fig. 1F). A wide spectrum of leukemic subtypes was identified, including AML, pre-T LBL, B-lineage ALL, erythroleukemia, and biclonal leukemia with concurrent pre-T LBL and AML (Fig. 1G and Supplementary Table S1).

AMLS showed a Mac1<sup>+</sup>/Gr1<sup>+</sup> population that infiltrated the BM, spleen, lymph nodes (not shown), thymus, and liver (Fig. 2). The Gr1<sup>+</sup> staining was relatively dim (Fig. 2A), as has previously been noted with immature granulocytes compared with mature granulocytes. A subpopulation of the AML cells were also B220<sup>+</sup> (Fig. 2A), a phenomenon previously recognized in AMLs that express NUP98-HOXD13 (16) or CALM-AF10 (17, 18) fusions. These cells were negative for CD19 and surface immunoglobulin M (sIgM; Fig. 2A, red arrows), demonstrating that they are not typical B220<sup>+</sup>/CD19<sup>+</sup> B cells. To further investigate B-lymphoid characteristics, we assayed 26 Mac1<sup>+</sup>/B220<sup>+</sup> AMLs for evidence of clonal *Igh* gene rearrangements and identified four samples with clonal DJ rear-

rangements (Supplementary Fig. S2A); none had evidence of a complete VDJ rearrangement. Histologic analysis showed extensive infiltration of the spleen and thymus, and a characteristic perivascular infiltration of the liver, with myeloperoxidase-positive (MPO<sup>+</sup>) cells (Fig. 2B). Leukemic tissues were negative for T-cell markers CD3, CD4, and CD8 (not shown). We established an immortal, cytokine-independent Mac1<sup>+</sup>/B220<sup>+</sup> cell line (designated 961C) from the BM of a mouse with AML; this cell line has now been passaged continuously for greater than 24 months. Most of the cells show a myeloblast morphology; however, a minor population of cells show a lower nuclear:cytoplasmic ratio and/or formation of ringed nuclei, morphologic findings suggestive of myeloid or monocytic differentiation (Supplementary Fig. S2B).

Pre-T LBLs were defined on the basis of the Bethesda proposals for classification of lymphoid neoplasm (19) and were typically CD4<sup>+</sup>/8<sup>+</sup> (Supplementary Table S1 and Supplementary Fig. S2C), with clonal *Tcrb* gene rearrangements (Supplementary Fig. S2D); expression of the NP23 fusion protein was documented by immunoblot (Supplementary Fig. S2E). The pre-T LBLs were invariably positive for cytoplasmic CD3<sup>+</sup> (cyCD3) by immunohistochemistry (IHC), but were not consistently surface CD3<sup>+</sup> by fluorescence-activated cell sorting (FACS) analysis (Supplementary Table S1), suggesting that some of the pre-T LBL were at the early cortical stage. Given that NOTCH1 mutations are common in both human and mouse pre-T LBL, we evaluated 10 pre-T LBL samples for *Notch1* mutation. Seven had acquired spontaneous mutations of the PEST, heterodimerization, or transmembrane domains (Supplementary Table S2). In addition, three of the seven also had a 5' deletion of *Notch1*, which leads to production of a truncated Notch1 protein and ligand-independent activation (20). *Hes1*, a target of NOTCH1, was consistently overexpressed in the pre-T LBLs but not in premalignant NP23 thymus (Supplementary Fig. S2F).

Many leukemias from the B10 line had both T-cell and myeloid features, suggesting that the leukemia was biclonal or biphenotypic. Varying proportions of discrete Mac1<sup>+</sup>/Gr1<sup>+</sup> and

## RESEARCH ARTICLE

Gough et al.

CD4<sup>+</sup>/CD8<sup>+</sup> populations were seen in BM, spleen, lymph node, and thymus (Supplementary Fig. S3Ai), suggesting that the leukemia was biclonal rather than biphenotypic. Immunohistochemical staining of the leukemic BM and liver suggests that the two populations are mutually exclusive, supporting the contention that the leukemia was biclonal (Supplementary Fig. S3Aii).

Five leukemic mice developed clonal CD19<sup>+</sup> B-cell malignancies (Supplementary Fig. S3B and S3C), and two mice developed erythroleukemia. Mouse 807 had erythroleukemia and presented with a markedly abnormal CBC [hemoglobin (Hgb), 1.9 g/dL; MCV, 77.9 fL; WBC, 0.6 K/ $\mu$ L; platelets, 31 K/ $\mu$ L] and a near-complete absence of myeloid cells in the BM (Supplementary Fig. S3D). The spleen showed replacement of B and T cells with immature Ter119<sup>dim</sup>/CD71<sup>+</sup> erythroblasts and a less prevalent population of more mature Ter119<sup>+</sup>/CD71<sup>dim</sup> cells, whereas the lymph node was infiltrated with immature Ter119 and a larger population of more mature nucleated red blood cells (not shown). Histologic sections show an effaced spleen infiltrated with Ter119<sup>+</sup> cells (Supplementary Fig. S3D).

In addition to the B10 and C10 lines, four additional founder mice developed leukemia (founders E6, G8, I2, and J5; Supplementary Table S1), demonstrating that the leukemias were not caused by a unique integration site effect in the B10 and C10 lines. To investigate why the C10 line primarily developed AML, whereas the B10 mice showed a wider array of leukemic subtypes, we assessed the age at diagnosis of leukemia, as well as the expression level of the transgene in different tissue types. The age of onset for the two major forms of leukemia observed in the NP23 mice (AML and pre-T LBL) was not significantly different (data not shown). Quantitative real-time PCR (qRT-PCR) showed *NP23* mRNA levels to be modestly higher in the C10 line in both the BM and thymus (Supplementary Fig. S3E), excluding the hypothesis that higher *NP23* expression levels in B10 thymus or in C10 BM might account for the variance in subtype frequency between the two founder lines.

### NP23 Mice Show Decreased Levels of HSPC and Impaired Differentiation

To determine whether the onset of leukemia was preceded by aberrant hematopoietic development, we compared HSPC from 4-month-old healthy NP23 mice (with no signs of hematologic disease) to those from WT littermate controls. FACS analysis demonstrated that the lineage-negative (Lin<sup>neg</sup>) compartment of the NP23 mice contained approximately half the absolute number of cells compared with WT BM (Supplementary Fig. S4Ai, iii). The Lin<sup>neg</sup>/Sca1<sup>+</sup>/cKit<sup>+</sup> (LSK) compartment, composed of functionally distinct long-term hematopoietic stem cell (LT-HSC), short-term HSC (ST-HSC), and multipotent progenitors, was dramatically reduced in the NP23 mice (Supplementary Fig. S4Aii, iv), and the absolute number of common myeloid progenitor, granulocyte-macrophage progenitor, and megakaryocyte-erythroid progenitors was also decreased (Supplementary Fig. S4Av). Despite the marked (>80%) reduction in BM LSK cell numbers and reduced early myeloid progenitors, a functional colony-forming cell (CFC) assay showed no decrease in the replating potential of the NP23 BM compared with WT or in the types of progenitor colonies formed (Supplementary Fig. S4Av,vi). In addition, NP23 BM showed a 2-fold increase in the unusual Mac1<sup>+</sup>/B220<sup>+</sup> population (Supplementary Fig. S4Avii).

NP23 thymi were smaller and contained 5-fold fewer thymocytes than WT controls (Supplementary Fig. S4B). Although FACS analysis suggested a relative increase in CD4/CD8 double-negative cells (DN) in the NP23 mice (Supplementary Fig. S4Bii), there was actually an absolute decrease in DN, CD4 and CD8 single-positive (SP), and, most markedly, in the CD4/CD8 double-positive (DP) thymocytes (Supplementary Fig. S4Biv). Further fractionation of the NP23 DN cells revealed a marked increase in the proportion of DN2 cells, reflecting a dramatic accumulation of cells in both the DN2a and DN2b populations, and a significant decrease in the DN3 and DN4 populations (Supplementary Fig. S4Biii,v). Taken together, these findings reflect a significant defect in normal thymocyte differentiation at the DN2 to DN3 transition, which likely contributes to the reduction of DP and SP thymocytes.

### NP23 Leukemias Overexpress *Hoxa* and *Hoxb* Genes

Gene expression profiles revealed that *Hoxa5/7/9* were among the most highly overexpressed genes in all three leukemic subtypes (Fig. 3A and Supplementary Tables S3 and S4), along with *Hoxb2/4/5/6/7/9*, *Meis1*, *Gpnmb*, *Nkx2-3*, and *Bahcc1* in AMLs; *Gm525*, *Gpnmb*, and *Bahcc1* in pre-T LBL; and *Vpreb1*, *Vpreb3*, and *Bahcc1* in B-ALL. The gene expression signatures found in the NP23 leukemic cells reflect abnormal regulation caused directly by the NP23 fusion product, as well as any dysregulation caused by undefined, collaborative mutations that arise spontaneously as the cell transforms. Therefore, to identify a gene expression signature caused solely by NP23 expression, we compared tissues from clinically healthy NP23 mice, which showed no evidence of malignancy, with those from WT littermates. NP23 BM, thymus, and spleen showed fewer differentially expressed genes than did the leukemias (Supplementary Table S6). Only five loci, *Hoxa5/7/9*, *Meis1*, and *Bahcc1*, were consistently overexpressed, suggesting that these were direct targets of the NP23 fusion protein, irrespective of hematopoietic cell type (Fig. 3B).

We validated overexpression of *Hoxa5/7/9/10* (hereafter referred to as the “*Hoxa* cluster”) by qRT-PCR. The more differentiated lineage-positive (Lin<sup>pos</sup>) WT BM cells showed a clear decrease of *Hoxa* cluster expression compared with undifferentiated WT Lin<sup>neg</sup> cells (Supplementary Fig. S5A). Importantly, this decrease was not seen in the NP23 Lin<sup>pos</sup> cells or AMLs. Overexpression of *Nkx2-3*, *Meis1*, *Hoxb5*, and *Mir196b*, a microRNA located between *Hoxa9* and *Hoxa10*, was likewise verified (Supplementary Fig. S5B). We also confirmed overexpression (3-fold to 76,000-fold) of the *Hoxa* cluster, *Mir196b*, and *Gm525* in the NP23 thymi, and pre-T LBLs (Supplementary Fig. S5C and S5D). Also consistent with the array data, *Meis1* expression was variable and not consistently overexpressed in the pre-T LBLs (Supplementary Fig. S5D).

### NP23-Associated Gene Expression Signatures Resemble Human HSPC and AML Subtypes

Gene set enrichment analysis (GSEA) showed the NP23 AML expression profile to be enriched in human HSPC (21) and AML (22) genesets (Fig. 3C and D). Leading-edge genes included *HOXA5/A7/A9*, *HOXB5/6/7*, and *MEIS1* (Fig. 3D and E). Additional genesets that overlapped with the NP23 AML expression signatures represented genesets associated with highly

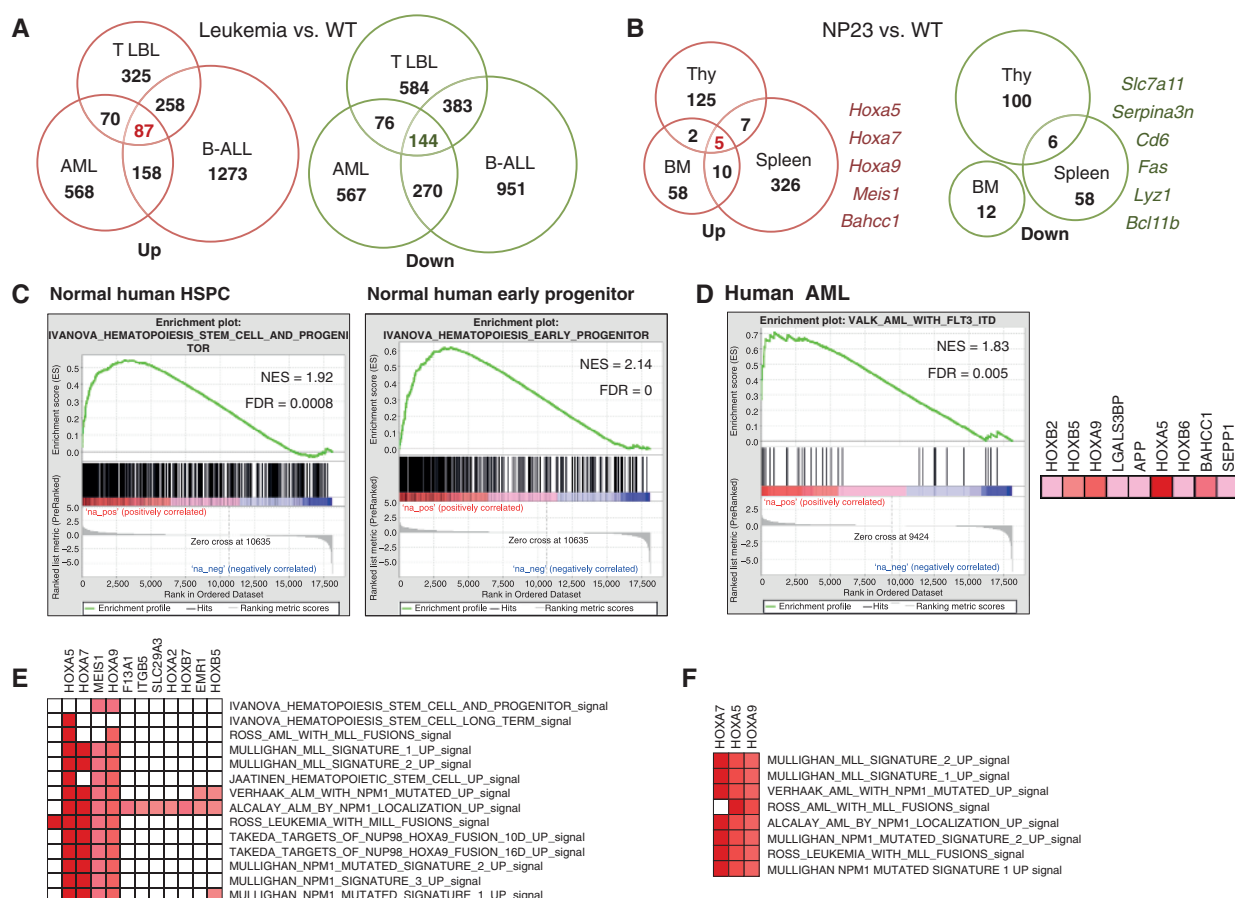


**Figure 3.** NP23 leukemias exhibit Hox/Meis1 stem cell-like gene expression signatures that are enriched in human HSPC and AML genesets. **A**, genes >1.5-fold overexpressed (red) or underexpressed (green) in AML, pre-T LBL, and pre-B-ALL compared with WT BM, thymus, or spleen (Supplementary Table S3). Eighty-seven genes were overexpressed and 144 decreased independent of tissue type (Supplementary Tables S4 and S5). **B**, genes >1.5-fold overexpressed (red) or underexpressed (green) in NP23 BM, thymus, or spleen compared with WT controls. Note a core set of only five genes are overexpressed irrespective of tissue type (Supplementary Table S6). **C**, enrichment profiles of genes overexpressed in NP23 AML (identified in Fig. 3A) compared to human HSPC and early progenitor genesets, and **D**, human AML; right panel, leading edge genes from the FLT3-ITD geneset. **E**, a subset of GSEA leading edge genes overexpressed in NP23 AML and enriched in human HSPC, early progenitor and AML genesets. **F**, leading edge genes overexpressed in NP23 pre-T LBL and enriched in human leukemic genesets. NES, normalized enrichment score; FDR, false discovery rate.

proliferative cells such as protein synthesis, modification, and metabolism, cell cycle, and DNA synthesis (data not shown). The pre-T LBLs similarly overexpressed *Hoxa* genes and demonstrated similarity with *MLL* and *NPM1* leukemic signatures (Fig. 3F).

### BAHCC1 Is Upregulated in Human Acute Leukemias Associated with HOXA Cluster Overexpression

Bromo adjacent homology (BAH) domain and coiled-coil containing 1 (*BAHCC1*), overexpressed in NP23 tissues, was also overexpressed in human AML (Fig. 4A). AML patient clusters 2 and 6 (22) showed markedly increased levels of *BAHCC1* compared with both normal BM and CD34 cells, whereas *HOXA9* and *MEIS1* were increased in both CD34 cells and AML samples, suggesting that *BAHCC1*, more so than *MEIS1* and *HOXA9*, is a specific marker for AML. Further analysis of *BAHCC1* expression in this dataset revealed overexpression in multiple patient clusters; interestingly, *BAHCC1* overexpression was

mutually exclusive with favorable prognosis AML [t(8;21), t(15;17) and inv(16); Fig. 4B]. Analysis of an independent dataset demonstrated that *BAHCC1* was also overexpressed in pre-B-ALL samples with *MLL* translocations [which also overexpress *HOXA* cluster genes (GSE33315); Fig. 4C; ref. 23]. Taken together, these findings suggest that *BAHCC1* may be a previously unsuspected marker for AML and pre-B-ALL associated with *HOXA* cluster gene expression.

### NP23 Directly Targets Both *Hoxa* and *Hoxb* Gene Clusters

Overexpression of numerous *Hox* genes in the NP23 transgenic mice and prior evidence of PHD finger binding of H3K4me2/3 active chromatin marks (15) suggest that H3K4me3 may be abnormally abundant at *Hox* and other genomic loci in the NP23 transgenic mice. We used H3K4me3 ChIP-seq to identify H3K4 methylation specific to NP23 leukemic cells. Comparison of H3K4me3 peaks from two NP23 pre-T LBL cell lines with that of a control non-NP23

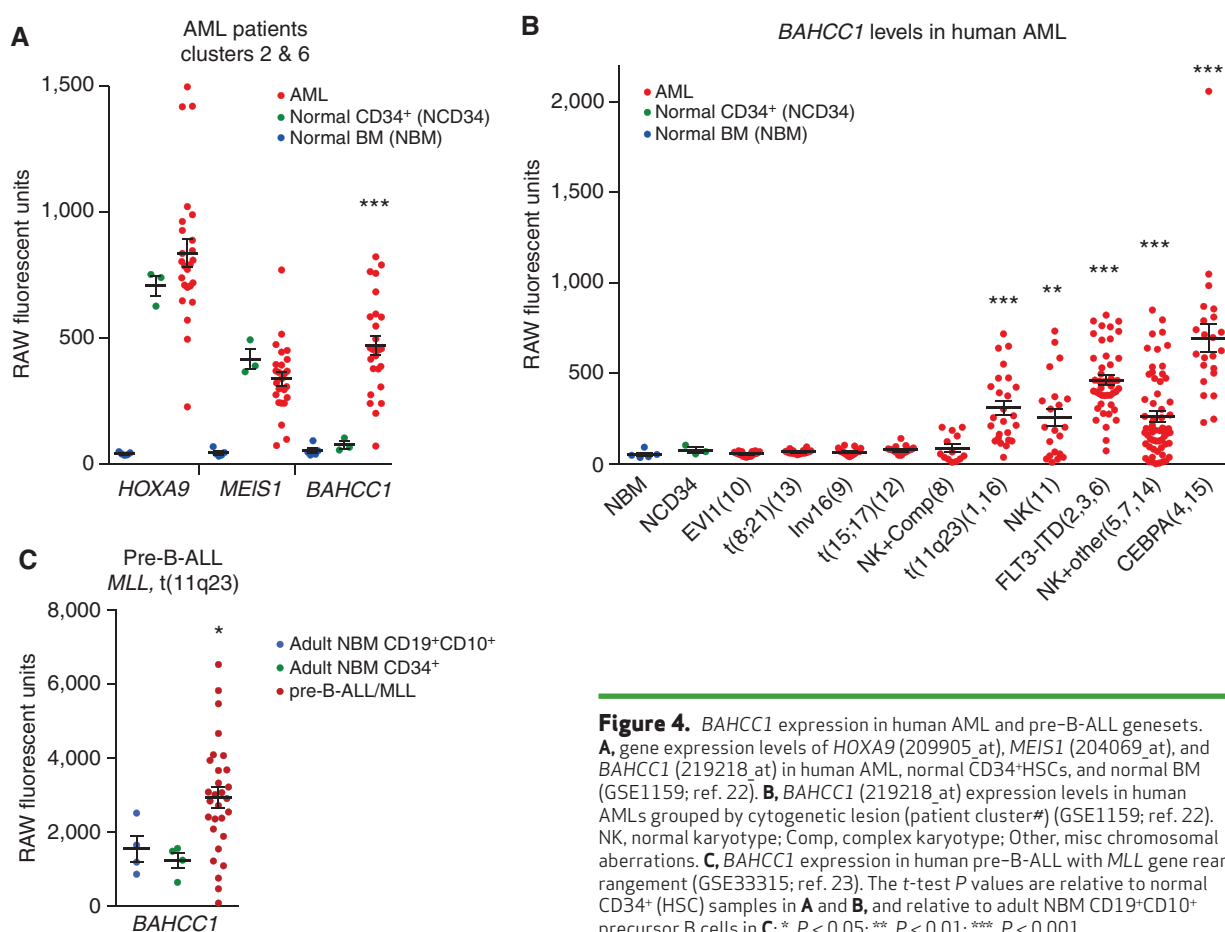


**Figure 4.** BAHCC1 expression in human AML and pre-B-ALL genesets. **A**, gene expression levels of HOXA9 (209905\_at), MEIS1 (204069\_at), and BAHCC1 (219218\_at) in human AML, normal CD34<sup>+</sup>HSCs, and normal BM (GSE1159; ref. 22). **B**, BAHCC1 (219218\_at) expression levels in human AMLs grouped by cytogenetic lesion (patient cluster#) (GSE1159; ref. 22). NK, normal karyotype; Comp, complex karyotype; Other, misc chromosomal aberrations. **C**, BAHCC1 expression in human pre-B-ALL with MLL gene rearrangement (GSE33315; ref. 23). The t-test P values are relative to normal CD34<sup>+</sup> (HSC) samples in **A** and **B**, and relative to adult NBM CD19<sup>+</sup>CD10<sup>+</sup> precursor B cells in **C**; \*, P < 0.05; \*\*, P < 0.01; \*\*\*, P < 0.001.

pre-T LBL cell line (7298/2; ref. 24) identified 429 H3K4me3 peaks shared by both NP23 pre-T LBL lines, but not the control cell line 7298/2 (Fig. 5A and Supplementary Table S7). Eighteen of the 429 enriched sites were at gene loci significantly overexpressed in NP23 pre-T LBL, including the highly overexpressed genes *Gm525* and *Hoxa* cluster genes (Fig. 5B and Supplementary Table S7). The NP23 T cells demonstrated a striking enrichment of H3K4me3 across the 5' *Hoxa* locus with a concurrent absence of H3K27me3 marks (Fig. 5C). In contrast, 7298/2 showed an inverse pattern of H3K4me3 and H3K27me3 enrichment.

To determine whether these ChIP-seq results were unique to the T cells, we performed ChIP-seq on the 961C myeloblast cell line. Similar H3K4me3 enrichment was identified across the 5' *Hoxa* locus in this cell line (Fig. 5D). ChIP-seq using an antibody to the NP23 fusion protein revealed remarkable colocalization with H3K4me3 marks, as 160 of 181 NP23-enriched loci were concomitantly H3K4me3 enriched (Fig. 5E and Supplementary Table S8). However, the NP23 protein was highly selective, as only 160 (1.6%) of the 9,863 H3K4me3-enriched sites bound NP23 (Fig. 5E and Supplementary Table S8). Comparison of genes overexpressed in NP23 AML samples with dual NP23+H3K4me3 sites of enrichment showed 18 loci in common (Fig. 5F and Supplementary Table S9). Four of these 18, *Hoxa7*, *Hoxa9*, *Meis1*, and *Hoxb5*, were also overexpressed in the healthy NP23 BM, suggesting that these four genes are early, direct targets of NP23, before transforma-

tion to AML (Fig. 5D, F, G, and H and Supplementary Table S9). Extensive H3K4me3 enrichment and binding of NP23 at the *Hoxb* locus, in conjunction with *Hoxb4/b5/b6/b7* overexpression in the NP23 BM and/or AMLs, suggests that *Hoxb* gene involvement is almost as extensive as the *Hoxa* cluster genes in the NP23 AML samples (Fig. 5H).

Of the five genes (*Hoxa5*, *Hoxa7*, *Hoxa9*, *Meis1*, and *Bahcc1*) overexpressed independent of lineage before transformation, *Bahcc1* stands in contrast to the others, as this locus is devoid of NP23 enrichment (Fig. 5I). Combined with the observation that BAHCC1 is overexpressed in a wide array of human AML and pre-B-ALL (Fig. 4), it seems reasonable to suggest that BAHCC1 overexpression is associated with HOXA/B gene expression signatures, but is not a direct target of the NP23 fusion.

### A Small Molecule That Inhibits H3K4me3 Binding by PHD Fingers Selectively Kills Cells That Express NUP98-PHD Oncoproteins

Given the coordinate upregulation of structurally similar proteins (HOXA5/7/9/10 and HOXB4/5/6/7) by NP23, targeting one or two of these proteins may have little effect on the transformed cell. However, inhibiting NP23 binding to H3K4me3 could potentially affect expression of the gene program. We evaluated five compounds (tegaserod, amiodarone, disulfiram, WAG-003, and WAG-004) that have recently been reported to inhibit PHD binding to H3K4me3 *in vitro* (25). All compounds were toxic at 200 μmol/L, the concentration used to

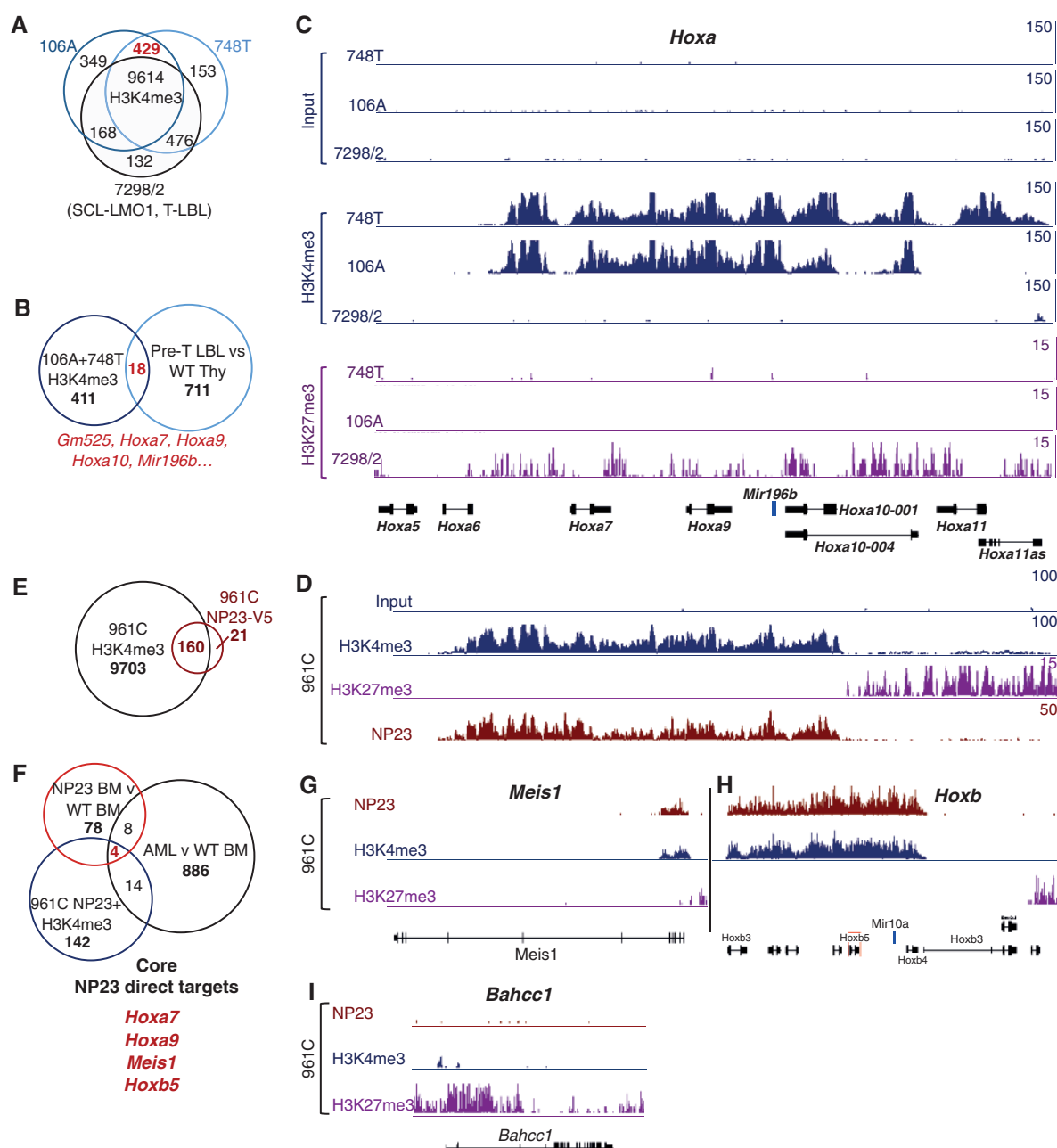


**Figure 5.** ChIP-seq identifies NP23-specific H3K4me3 enrichment and direct NP23 targets genome-wide. **A**, H3K4me3-enriched genes in two NP23 pre-T LBL-derived cell lines 106A and 748T, compared with H3K4me3-enriched genes in a non-NP23 control pre-T LBL cell line (murine SCL-LMO1 cell line 7298/2). Four hundred twenty-nine sites were specific to NP23 106A and 748T (Supplementary Table S7). **B**, overlap of NP23 T-cell H3K4me3-enriched genes and genes overexpressed in pre-T LBL. **C**, H3K4me3 and H3K27me3 ChIP-seq at the 5'-*Hoxa* locus in 106A and 748T, compared with control cell line 7298/2. **D**, H3K4me3, H3K27me3, and NP23 ChIP-seq at the 5'-*Hoxa* locus of the NP23 AML-derived myeloblastic cell line 961C. **E**, NP23 targets only 160 (1.6%) of the 9,863 H3K4me3-enriched sites at annotated genes genome-wide (Supplementary Table S8). **F**, comparison of genes with dual NP23 and H3K4me3 enrichment to genes overexpressed in AML and healthy NP23 BM (Supplementary Table S9). *Hoxa7*, *Hoxa9*, *Meis1*, and *Hoxb5* are overexpressed in both healthy NP23 BM and NP23 AML, and are direct targets of NP23. H3K4me3, H3K27me3, and NP23 ChIP-seq at *Meis1* (**G**), the *Hoxb* locus (**H**), and at *Bahcc1* (**I**). Note, *Bahcc1* is void of NP23 binding.

demonstrate inhibition of histone reader function *in vitro* (25); however, only disulfiram was toxic to the NP23 myeloblast and lymphoblast cell lines (961C and 748T, respectively) at the lowest (2 μmol/L) concentration initially tested (Supplementary Fig. S6A). We focused on the myeloid lineage as NUP98-PHD fusions have been found exclusively in patients with AML to

date, and next evaluated the ability of lower concentrations of disulfiram to inhibit proliferation of the 961C cell line, treated in parallel with two non-NP23 myeloblast control cell lines, 189E6 and 32D. 961C showed the greatest sensitivity to disulfiram, which selectively killed 961C cells at 2 and 0.66 μmol/L, while controls 189E6 and 32D continued to proliferate

(Supplementary Fig. S6B). As early as 6 hours after treatment, 961C cells showed apoptotic changes (Fig. 6A), and by 24 hours, 100% of disulfiram-treated 961C cells were dead. To extend these observations, we evaluated an independent AML cell line (NJL) driven by the leukemic fusion gene *NUP98-JARID1A* (*NJL*), which contains a PHD motif that similarly “reads” H3K4me3 marks. Disulfiram was similarly toxic to NJL cells (Fig. 6). In contrast, four control myeloid leukemia cell lines (188G3, 189E6, 32D, and Ba/F3) showed little or no increase in apoptosis compared with vehicle-treated cells (Fig. 6B).

We hypothesized that disulfiram would inhibit NP23 binding at critical NP23 target genes (*Hoxa* cluster, *Hoxb* cluster, and

*Meis1*), resulting in decreased expression of these genes and subsequent cell death. Following treatment of 961C cells, we observed significant decreases in the binding of NP23 to *Hoxa7*, *Hoxa9*, *Hoxa10*, *Meis1*, *Hoxb5*, and *Mir196b* target genes (Fig. 7A and B). *Gapdh*, a non-NP23 target (not bound by NP23 but enriched for H3K4me3; Supplementary Table S8), showed little to no enrichment compared with input, as expected. In contrast to decreased NP23 binding, H3K4me3 marks remained stable, as did chromatin-bound RNA polymerase II (Fig. 7A), indicating a specific effect of disulfiram on the NP23-chromatin (H3K4me3) interaction. In addition, *Hoxa7* mRNA levels decline as early as 3 hours following disulfiram exposure, and by 6 hours after treatment, mRNA levels

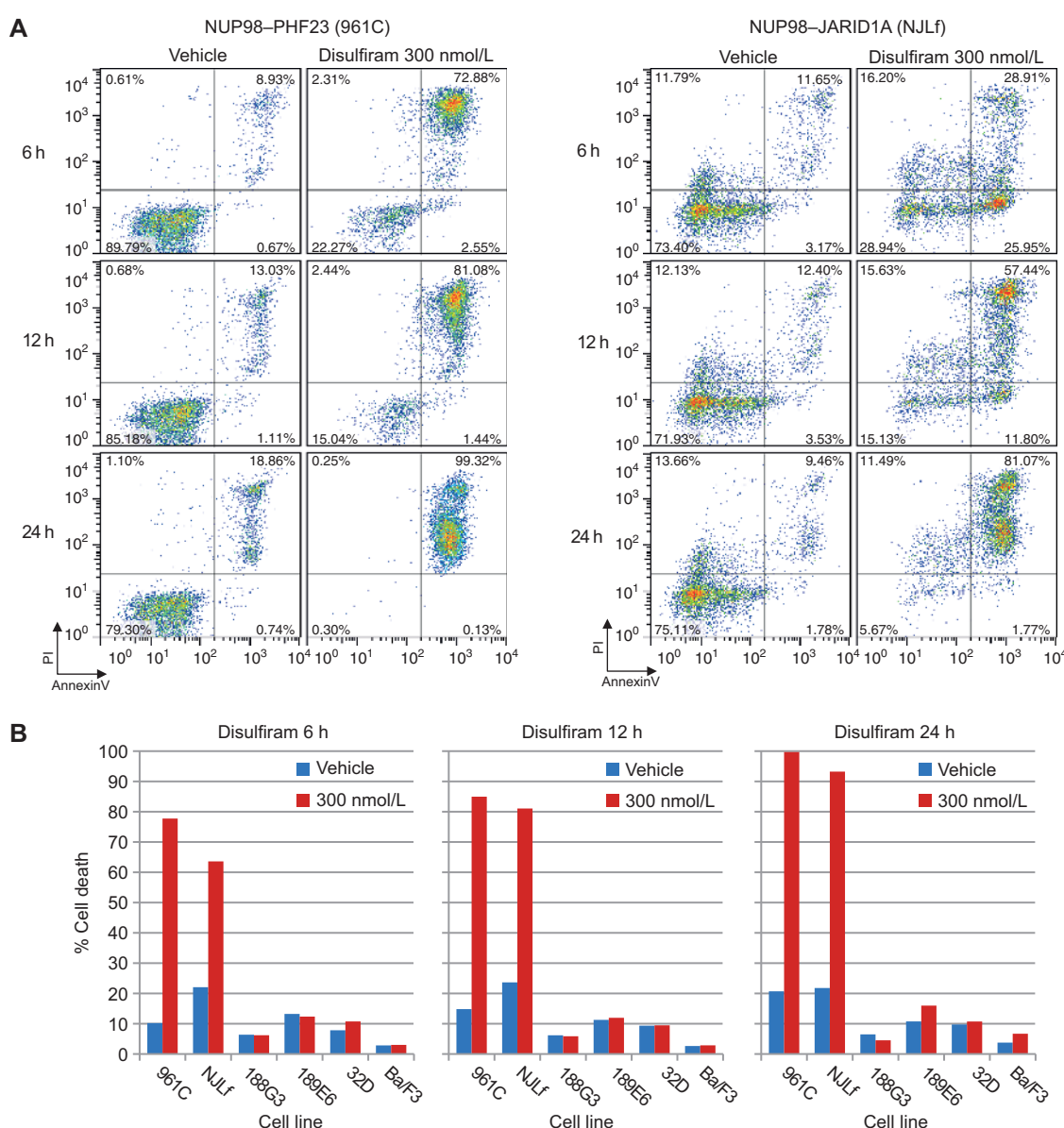


**Figure 6.** Disulfiram selectively kills leukemic cells driven by H3K4me3-binding NUP98-PHD fusions. **A**, apoptotic (PI<sup>+</sup>/Annexin V<sup>+</sup>) analysis of NP23 (961C) and NJL AML cell lines at 6, 12, and 24 hours following treatment with 300 nmol/L disulfiram or vehicle (dimethyl sulfoxide). **B**, graphed proportions of apoptotic/dead cells shown in **A**. Early apoptotic, late apoptotic, and necrotic cell populations are combined to represent “% cell death” in NUP98-PHD cell lines 961C and NJL, compared with AML control (non-NP23) cell lines 188G3 (NUP98-HOXD13), 189E6 (NUP98-HOXD13), 32D, and Ba/F3. Representative of three independent experiments. PI, propidium iodide.

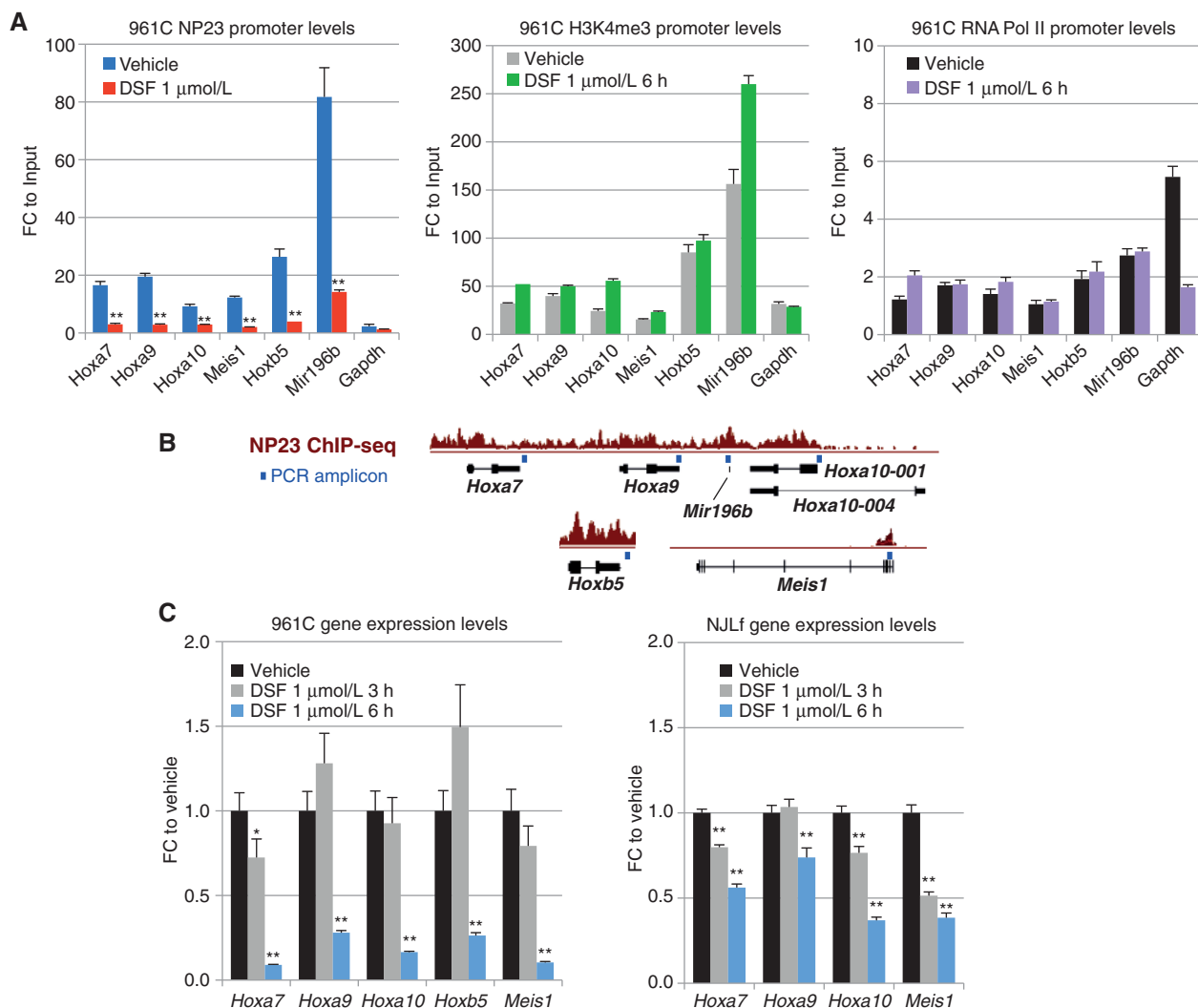


**Figure 7.** Disulfiram treatment leads to reduced NP23 chromatin binding and target gene expression. **A**, ChIP of promoter-associated NP23 fusion protein at target loci and *Gapdh* in 961C cells after 6 hours disulfiram (DSF) treatment (1 μmol/L). NP23 (left), H3K4me3 (middle), and RNA polymerase II (right) levels. **B**, ChIP qPCR amplicon locations (blue square) are indicated relative to target gene and NP23 ChIP-seq tracks (as shown in Fig. 5). **C**, qRT-PCR quantification of mRNA transcripts of target genes *Hoxa7*, *Hoxa9*, *Hoxa10*, *Hoxb5* (not expressed in NJLf), and *Meis1* in 961C (left) and NJLf (right) cells treated with disulfiram compared with vehicle (dimethyl sulfoxide)-treated cells.  $C_t$  values were normalized to internal ribosomal controls. P values are relative to vehicle control. Error bars, SEM; t test P values are indicated; \*,  $P < 0.05$ ; \*\*,  $P < 0.01$ .

of all NP23 target genes assayed were decreased (Fig. 7C). Similar reductions in mRNA transcripts were observed in NJLf cells treated with disulfiram (Fig. 7C). We propose that inhibition of NP23 and NJL binding to H3K4me3, via their PHD motifs, leads to failure of these NUP98-PHD fusion proteins to “read” and maintain expression of critical target genes, resulting in subsequent silencing of multiple gene targets and rapid apoptotic cell death.

## DISCUSSION

The *NP23* fusion is potently oncogenic *in vivo*, causing acute leukemias of myeloid, T- and B-lymphocyte, and erythroid origin, with a latency suggesting that collaborative mutations are required for transformation. This range of leukemic subtypes was identified in six founders and their offspring, indicating that the leukemias were not caused by a unique transgene

insertion site. The AMLs were typically Mac1<sup>+</sup>/Gr1<sup>+</sup>/B220<sup>low</sup>, similar to those described for the *NUP98-HOXD13* and *CALM-AF10* murine models (17, 18, 26). Clonal DJ Ig $\beta$  gene rearrangements were detected in a small proportion (4 of 26) of the Mac1<sup>+</sup>/B220<sup>+</sup> AMLs, which has also been seen in patients with biphenotypic leukemia (27) and in the CALM-AF10 murine model (18). Pre-T LBLs were typically immature CD4/CD8 DP with clonal *Tcrb* rearrangements and *Notch1* mutations, consistent with previously described murine T LBL models (28, 29) and human T-ALL (30, 31). Erythroid and B-ALL leukemias were less common and characteristically Ter119<sup>+</sup> and CD19<sup>+</sup> with clonal Ig $\beta$  rearrangement, respectively.

NP23 mice show evidence of impaired HSPC development and differentiation in multiple hematopoietic lineages before the onset of leukemia, consistent with previous studies of *NUP98* fusion genes (1). Young, healthy NP23 mice showed

## RESEARCH ARTICLE

## Gough et al.

dramatic reductions in HSPCs, most notably within the LSK fraction. In addition, there was a clear decrease in thymocyte number in the NP23 mice, at least in part due to a differentiation block at the DN2 stage. However, despite a significant reduction in BM HSPC numbers, there was no decrease in the number of CFCs in NP23 BM compared with that of WT BM. Taken together, these observations are consistent with a model in which a subpopulation of NP23 hematopoietic cells are endowed with an increased capacity for self-renewal, but are resistant to orderly hematopoietic differentiation.

Impaired differentiation of NP23 hematopoietic cells is consistent with overexpression of the 5' *Hoxa* gene cluster (*Hoxa5/a7/a9/a10*, including *Mir196b*) and *Meis1* in NP23 hematopoietic tissues. Reduction of *Hoxa/Meis1* expression is necessary for normal hematopoietic differentiation (32), and persistent expression of these genes maintains a stem cell-like gene expression program that impairs differentiation. Changes in gene expression patterns in hematopoietic tissues from healthy NP23 mice reflect direct effects of the NP23 fusion protein before the acquisition of collaborating mutations and malignant transformation. Indeed, we see relatively few alterations in the gene expression signatures of NP23 hematopoietic tissues compared with abnormalities of the NP23 leukemic tissues (Fig. 3A and B); however, the few changes that do occur include marked upregulation of the 5' *Hoxa* genes, the *Hoxa9*cofactor *Meis1*, and the *Bahcc1* gene. We conclude that an early consequence of the NP23 fusion is the dysregulation of these key genes, and is in keeping with the enhanced self-renewal seen in the NP23 BM despite the reduced progenitor numbers. We propose that the seemingly discordant observations of reduced progenitor numbers and increased self-renewal could be explained by higher ratios of NP23 progenitors being capable of self-renewal, for more cycles, than the equivalent WT BM progenitors.

The 5'-*Hoxa* stem cell-like gene expression signature and elevated levels of *Bahcc1* were maintained in the AML, pre-T LBL, and B-ALL malignancies, with additional overexpression of *Meis1* and *Hoxb* genes (*b2/b4/b5/b6/b7/b9*) in the AML and the B-ALL (*Hoxb5/b7/b9*). Additional genes overexpressed in the NP23 leukemias include *Stat5a*, which is important in HSC self-renewal and differentiation programs and a cofactor of the HOXA9/MEIS1 transcription activation complex (33, 34). Homeobox transcription factor genes *Nkx2-3* and *Hhex* are significantly elevated, and have been reported to be overexpressed in human AML and pre-T LBL (35, 36). Like the *Hox* genes, *Hhex* is normally highly expressed in the HSPC compartment and subsequently downregulated during normal T-cell development (35). *Bmi1*, which is expressed in normal stem cell gene expression programs and is deregulated in human leukemias (37), was also elevated in the AML, T-, and B-cell NP23 leukemias. Tissue-specific differences in aberrant gene expression were also detected in leukemic samples from NP23 mice. Notably, *Meis1* was markedly increased in the AML samples, but was not elevated in the pre-T LBL samples. *Vpreb1* and *Vpreb3*, which are normally expressed in immature B cells and human B-cell precursor ALL, were increased in the B-ALL samples from the NP23 mice (38).

There were a number of poorly characterized transcripts overexpressed in the NP23 leukemias (*1810015a11rik*, *2010111i01rik*, *4930539e08rik*, *4930452B06Rik*, *5330431n19rik*, *Bc003885*, *Bc025076*, *E130012a19rik*, *Eg277333*, *Gm525*, *Gm885*,

and *Loc65446725*), one of which, *Gm525*, was the single most highly overexpressed gene in the NP23 pre-T LBL. The human homolog, *C17orf67*, is expressed in normal fetal thymus tissue (GO GDS786), but little more is known about this transcript (39). In addition, a number of gene families were overexpressed in the AML, pre-T LBL, and B-ALL. These included *Psmb1*, *Psmb8*, *Psmb9* (proteosome protein processing), *Cenpa*, *Cenpl*, *Cenpk*, *Cenph*, *Cenpp*, *Incenp* (centromere/kinetochore function), *Hist1h2ag*, *Hist1h2ao*, *Hist1h2an*, *Hist1h2ab*, *Hist2h2ac* (replication-dependent histone mRNAs of the H2A histone family), *H2afy* (H2A histone family), *Kif22*, *Kif15*, *Kif18a* (kinesin family—microtubule-associated molecular motors), *Chaf1a*, and *Chaf1b* (subunits of chromatin assembly factors that assemble histone octamers onto replicating DNA), genes that are typically expressed in rapidly dividing cells.

No genes were consistently downregulated in all three healthy NP23 hematopoietic tissues. Genes downregulated in AML were largely dominated by the loss of transcripts associated with erythropoiesis, reflecting the phenotype of the homogeneous leukemia compared with a mixed population of cells in WT BM. A number of *Klf* family members were significantly decreased (*Klf1*, *Klf2*, *Klf4*, *Klf5*, *Klf6*, and *Klf7*) in the NP23 leukemias. *Klf* genes encode transcription factors, some of which function in hematopoietic proliferation and differentiation and can act as tumor suppressors (40).

We found NP23 AML expression signatures to be enriched in a number of normal human HSPC and AML gene expression profiles, most notably those with *MLL* and *NPM1* mutations. The pre-T LBL and B-ALL gene profiles were similarly enriched in human HSPC signatures, and showed additional similarity to T-cell and B-cell signatures, respectively. The unbiased approach taken here to screening gene expression pre- and post-transformation identified *Bahcc1* overexpression as an early event, closely associated with aberrant *Hoxa* gene expression. Of note, this observation was recapitulated in specific genetically defined subsets of human AML. *BAHCC1* was dramatically elevated in a subset of human AML samples, but, in contrast to *HOXA9* and *MEIS1*, was not elevated in immature CD34<sup>+</sup> cells, suggesting that *BAHCC1* overexpression may be a more specific indicator of leukemic transformation than *HOXA9* or *MEIS1*. Higher levels of *BAHCC1* expression were associated with AML that had an *MLL* rearrangement [t(11q23)], FLT3-ITD, CEBPA, or normal karyotype; most of these subtypes have previously been associated with *HOXA* gene overexpression and a poor prognosis. Pre-B-ALL with *MLL* rearrangement similarly showed elevated *BAHCC1*. Our observations suggest that *BAHCC1* overexpression may be a useful early marker for leukemic transformation.

Epigenetic modifications of histones, especially H3K4me3 and H3K27me2/3, are thought to be key regulators of gene expression and have gained increased interest as markers and targets for cancer therapy (11, 41). We identified specific sites of H3K4me3 enrichment in the myeloid and T-cell lines that correlated with the gene expression profiles of the AML and pre-T LBL malignancies. Notably, the *Hox* loci did not show the “bivalent” pattern described in embryonic stem (ES) cells (42), thought to facilitate dynamic transcriptional regulation during various stages of development, but showed abundant H3K4me3, not only at promoter regions but also spreading along the length of the gene, and were devoid of H3K27me3,

suggesting a more rigid, forced activation of these genes in the NP23 leukemias. Furthermore, we determined genome-wide NP23 binding sites, and discovered NP23 binding to be quite specific, binding only 1.6% of H3K4me3-enriched sites; this specificity suggests the involvement of an unknown cofactor(s) that helps direct NP23 target binding. NP23 was preferentially bound to numerous genes that were overexpressed in the AML samples; these genes included the 5' *Hoxa* cluster, several *Hoxb* genes, and *Meis1*. These observations support the hypothesis that NUP98-PHD fusions impose aberrant chromatin modifications by binding and potentially preserving H3K4me3 marks to maintain and promote active gene transcription. Because the normal targets for PHF23 are currently unknown, it remains unclear whether the NP23 fusion aberrantly activates normal PHF23 targets, or retargets the PHD of PHF23 to an alternate set of target sites. Notably, *Bahcc1* was not a direct target of NP23, which is consistent with our observations of elevated *BAHCC1* levels in numerous human leukemias, including those without an *NP23* fusion. Little is known about *BAHCC1*, but related BAH domain-containing proteins have been reported to function in chromatin regulation (protein-protein interactions, histone methyl-lysine binding; ref. 43).

The epigenetic nature of the NP23-imposed stem cell-like gene expression program suggests that direct effects of the fusion protein may be reversible and therefore may represent an attractive target for therapeutic intervention. We evaluated five compounds that have recently been reported to inhibit binding of H3K4me3 PHD histone readers. Of these five, disulfiram showed dramatic and selective killing of the NP23 myeloblast cell line, with no evidence of increased cell death in four different control myeloblast cell lines. Disulfiram was originally developed and is U.S. Food and Drug Administration (FDA)-approved for the treatment of alcoholism. However, based on anecdotal reports of antitumor activity in patients with cancer receiving the drug as treatment for coexisting alcohol addiction, disulfiram is now being investigated as a potential anticancer agent (44). Importantly, the concentration used in our studies (300 nmol/L and 1 μmol/L) is below clinically achievable peak levels (45).

Disulfiram treatment resulted in a rapid and complete apoptotic death of the NP23 cells, which was preceded by a reduction of NP23 levels at representative target promoters, suggesting that disulfiram inhibits NP23 binding of H3K4me3 residues *in vivo*. Gene expression was decreased as early as 3 hours after treatment, and dramatically reduced by 6 hours after exposure, in both 961C and NJLF cells. We propose that inhibition of NP23 and NJL binding to H3K4me3 via their PHD motifs leads to failure of these NUP98-PHD fusions to "read" and maintain expression of their target genes, resulting in rapid downregulation of target genes and apoptotic cell death. Given that there was no decrease in H3K4me3 and RNA polymerase II levels on target genes after disulfiram treatment, we suggest that the mechanism by which decreased NP23 binding might affect transcription of target genes may be via disruption of transcriptional cofactor recruitment (i.e., p300 and CBP) by the NUP98 amino terminus (1, 46). We hypothesize that the rapid and dramatic killing effect is due to the simultaneous downregulation of multiple targets.

We have shown that the NUP98 fusion protein NP23 is oncogenic in multiple cell types, including myeloid, eryth-

roid, T-lymphocyte, and B-lymphocyte. A common theme in all NP23 leukemias was enforced expression of *Hoxa* cluster genes and *Mir196b*, a microRNA embedded in the *Hoxa* cluster, suggesting that expression of this gene cluster is a strongly oncogenic, final common pathway in hematopoietic cells, irrespective of specific cell type. Treatment of NP23 cells with a known inhibitor of H3K4me3 PHD binding led to reduced chromatin-bound NP23 protein, inhibition of *Hoxa* cluster and *Meis1* expression, and rapid apoptosis of NP23 cells. In addition, transformed cells containing a related NUP98-PHD fusion (NJL) were likewise selectively killed by disulfiram, and also demonstrated reduction of *Hoxa* cluster and *Meis1* expression. These findings suggest that inhibition of the NP23 PHD binding to H3K4me3 may be an effective and specific treatment of NP23 leukemias, and, by extension, other leukemias driven by H3K4me3 "readers."

## METHODS

### Generation of Transgenic NP23 Mice

The *NP23* fusion gene has previously been described (Fig. 1A; ref. 14). PCR primers were used to introduce *Sfi*I and *Not*I restriction sites, as well as a C-terminal V5 epitope tag, into the *NP23* transgene construct (Supplementary Fig. S1A and Supplementary Table S10). This PCR product was subcloned into the *Sfi*I and *Not*I sites of the HS21/45-vav vector (47), placing the expression of the fusion gene under the control of hematopoietic-specific *Vav* regulatory elements. Founders were generated by injection of the purified *Pmel*-released fragment from p898/NP23-2 containing *Vav1-NP23-V5-vav2* into C57BL/6 zygotes. Positive *NP23* founder mice were bred with WT C57BL/6, and pups were genotyped for the *NP23* transgene by PCR with the forward and reverse primers NUPPHF(C)F and PHF23R1 (Supplementary Fig. S1A and Supplementary Table S10). WT controls were age-matched littermate controls. Animal studies were approved by the National Cancer Institute (NCI) Intramural Animal Care and Use Committee. Evaluation of mouse health is described in Supplementary Methods.

### PCR

PCR was performed using HiFi Taq polymerase mix (Invitrogen) and primers (Invitrogen) as listed in Supplementary Table S10. Clonal *Igb* DJ or VDJ segments were identified by PCR (48). Lin<sup>neg</sup> cells were purified by negative selection with StemSep Mouse Hematopoietic Progenitor Kit Lineage Positive antibody cocktail (STEMCELL Technologies) using the manufacturer's recommended protocol and MACS Separation Columns (Miltenyi Biotech Inc.). RNA was extracted using TRIzol (Invitrogen) or Qiagen RNeasy Kit (Qiagen) using the manufacturer's recommended protocol. cDNA was generated by RT-PCR using 1 μg RNA in 20 μL final volume with SuperScript III (Invitrogen) and diluted at 1:1 with water. qRT-PCR was performed with TaqMan primer-probe sets and ABI Fast Universal PCR Master Mix on an ABI Fast7500 system (Applied Biosystems/Life Technologies). Samples were normalized to endogenous 18S rRNA using TaqMan Ribosomal RNA Control Reagents. The *NP23* fusion gene was quantified using ABI Power SYBR Green Master Mix (ABI/Life Technologies) and PHF23 R2 and NUPPHF(C)F primers.

### Southern Blot Analyses of *Tcrb* and *Igh* Gene Rearrangements

High molecular weight genomic DNA for Southern blots was extracted by standard salting-out procedures (24) or Qiagen Blood and Tissue DNA Extraction Kit (Qiagen). *Tcrb* and *Igh* Southern hybridization procedures were performed as described previously (17).

## RESEARCH ARTICLE

Gough et al.

**Flow Cytometry, IHC, and Immunoblotting**

FACS analysis was performed as described elsewhere (16) with the following conjugated antibodies: Mac1-phycerythrin (PE), Gr1-fluorescein isothiocyanate (FITC), B220-allophycocyanin (APC), B220-FITC, CD19-PE, surface IgM-PE, CD43-FITC, CD3-PE, CD4-APC, CD8-FITC, CD71-PE, Ter119-FITC, Sca-1-PE, cKit-FITC, cKit-APC-Cy7, IL-7Ra-PE-Cy7, CD34-FITC, and CD16/32-PE (eBiosciences or BD Biosciences). StemSep Mouse Hematopoietic Progenitor Kit Lineage-Positive antibody cocktail (STEMCELL Technologies, Vancouver, Canada) was used to detect Lin<sup>pos</sup> BM cells, stained as previously described (16). Apoptosis assays were conducted using Annexin V-FITC Apoptosis Detection Kit I following the manufacturer's recommended protocol. IHC and immunoblotting were performed as previously described (49). Formalin-fixed paraffin-embedded sections were stained with hematoxylin and eosin (H&E), MPO (A0398; Dako), CD3 (MCA1477; AbD Serotec), B220 (553086; BD Biosciences), and Ter119 (116201; BioLegend). Stained slides were scanned and imaged as described elsewhere (49). For immunoblots, primary antibodies used were anti-V5 (ab9116, Abcam or R960-25, Life Technologies) and β-actin (Cell Signaling Technology). Protein was visualized using Pierce ECL Western Blotting Substrate (Thermo Scientific) and Amersham Hyperfilm ECL (GE Healthcare Ltd.).

**Cell Culture, Cell Lines, and Small-Molecule PHD Inhibitor Assays**

NP23 cell lines (106A, 748T, 1057d, and 961C) were established from single-cell suspensions prepared from BM ( $1 \times 10^6$  cells) and maintained in Iscove's Modified Dulbecco's Medium (IMDM) supplemented with 20% FBS, 100 mmol/L L-glutamine, and 100 µg/mL penicillin/streptomycin (Invitrogen). 7298/2 (24) was maintained in the same media. The myeloid leukemia cell line immortalized by NJL (NJLf) was generated as described previously (15) and maintained as for NP23 lines but with the cytokines murine stem cell factor (mSCF; 10 ng/mL) and murine interleukin-3 (mIL-3; 5 ng/mL). The 188G3 and 189E6 myeloblastic cell lines were derived from ES cells transformed with the NUP98-HOXD13 fusion gene (50) and maintained as for NP23 cell lines with 10 ng/mL mIL-3 (Peprotech). The Ba/F3 and 32D (clone 3) cell lines were purchased from American Type Culture Collection and maintained in RPMI supplemented with 15% FBS, 100 mmol/L L-glutamine, 100 µg/mL penicillin, 100 µg/mL streptomycin, and 10 or 5 ng/mL mIL-3, respectively. NP23 BM colony-forming unit (CFU) assays were performed using MethoCult GF M3434 (STEMCELL Technologies; www.stemcell.com). Small-molecule PHD inhibitors tetraethylthiuram disulfide (disulfiram; Sigma), amiodarone HCL (Sigma), tegaserod maleate (Sigma), and amiodarone analogs WAG-003 and WAG-004 (25) were solubilized in dimethyl sulfoxide (DMSO; Sigma). Cells were seeded at  $2 \times 10^5$ /mL for drug treatment assays.

**Gene Expression Profiling**

Tissues were analyzed using Illumina MouseRef-8 v2.0 Expression BeadChips (Illumina). Details are described in Supplementary Methods. This gene expression dataset can be accessed at National Center for Biotechnology Information's (NCBI) Gene Expression Omnibus (GEO) under accession number GSE54787.

**ChIP and ChIP-Seq**

ChIP was performed using a ChIP-IT kit from Active Motif following the manufacturer's recommended protocol with minor modifications as described in Supplementary Methods. Antibodies used were anti-H3K4me3 (17-614; Millipore), anti-H3K27me3 (07-449; Millipore), anti-V5 (R960-25; Life Technologies), anti-FLAG (M2; Sigma-Aldrich), and anti-RNA polymerase II (CTD4H8; Santa Cruz Biotechnology). This ChIP-seq dataset can be accessed under GEO accession number GSE54786.

**Disclosure of Potential Conflicts of Interest**

J.M. Denu is a consultant to Sirtris-GlaxoSmithKline. No potential conflicts of interest were disclosed by the other authors.

**Authors' Contributions**

**Conception and design:** S.M. Gough, Y. Ning, P.D. Aplan

**Development of methodology:** S.M. Gough, F. Yang, R.L. Walker, G.G. Wang, P.D. Aplan

**Acquisition of data (provided animals, acquired and managed patients, provided facilities, etc.):** S.M. Gough, F. Lee, F. Yang, M. Pineda, M. Onozawa, E.K. Wagner, B. Xu, P.S. Meltzer

**Analysis and interpretation of data (e.g., statistical analysis, biostatistics, computational analysis):** S.M. Gough, F. Lee, Y.J. Zhu, M. Onozawa, Y.J. Chung, S. Bilke, P.S. Meltzer, P.D. Aplan

**Writing, review, and/or revision of the manuscript:** S.M. Gough, E.K. Wagner, J.M. Denu, P.S. Meltzer, P.D. Aplan

**Administrative, technical, or material support (i.e., reporting or organizing data, constructing databases):** S.M. Gough, R.L. Walker, Y.J. Chung, G.G. Wang

**Study supervision:** S.M. Gough, P.D. Aplan

**Provided small molecule inhibitors:** J.M. Denu

**Acknowledgments**

The authors thank Michael Kuehl, Jay Hess, Sandy Morse, and current and former members of the Aplan laboratory for insightful discussions. The authors also thank Maria Jorge for expert assistance with animal care and husbandry, the NCI Transgenic Core facility for the generation of the NP23 transgenic mice, and the NCI Sequencing core for Sanger sequencing.

**Grant Support**

This work was supported by the Intramural Research Program of the National Cancer Institute, National Institutes of Health (grant numbers ZIA SC 010378 and BC 010983).

Received July 23, 2013; revised February 10, 2014; accepted February 11, 2014; published OnlineFirst February 17, 2014.

**REFERENCES**

1. Gough SM, Slape CI, Aplan PD. NUP98 gene fusions and hematopoietic malignancies: common themes and new biological insights. *Blood* 2011;118:6247–57.
2. Lisboa S, Cerveira N, Bizarro S, Correia C, Vieira J, Torres L, et al. POU1F1 is a novel fusion partner of NUP98 in acute myeloid leukemia with t(3;11)(p11;p15). *Mol Cancer* 2013;12:5.
3. Hollink IH, van den Heuvel-Eibrink MM, Arentsen-Peters ST, Prat-corona M, Abbas S, Kuipers JE, et al. NUP98/NSD1 characterizes a novel poor prognostic group in acute myeloid leukemia with a distinct HOX gene expression pattern. *Blood* 2011;118:3645–56.
4. Pineault N, Buske C, Feuring-Buske M, Abramovich C, Rosten P, Hogge DE, et al. Induction of acute myeloid leukemia in mice by the human leukemia-specific fusion gene NUP98-HOXD13 in concert with Meis1. *Blood* 2003;101:4529–38.
5. Wang GG, Cai L, Pasillas MP, Kamps MP. NUP98-NSD1 links H3K36 methylation to Hox-A gene activation and leukaemogenesis. *Nat Cell Biol* 2007;9:804–12.
6. Ferrando AA, Armstrong SA, Neuberg DS, Sallan SE, Silverman LB, Korsmeyer SJ, et al. Gene expression signatures in MLL-rearranged T-lineage and B-precursor acute leukemias: dominance of HOX dysregulation. *Blood* 2003;102:262–8.
7. Golub TR, Slonim DK, Tamayo P, Huard C, Gaasenbeek M, Mesirov JP, et al. Molecular classification of cancer: class discovery and class prediction by gene expression monitoring. *Science* 1999;286:531–7.

8. Soulier J, Clappier E, Cayuela JM, Regnault A, Garcia-Peydro M, Dombret H, et al. HOXA genes are included in genetic and biologic networks defining human acute T-cell leukemia (T-ALL). *Blood* 2005;106:274–86.
9. Armstrong SA, Staunton JE, Silverman LB, Pieters R, den Boer ML, Minden MD, et al. MLL translocations specify a distinct gene expression profile that distinguishes a unique leukemia. *Nat Genet* 2002;30:41–7.
10. Wang GG, Allis CD, Chi P. Chromatin remodeling and cancer, part I: covalent histone modifications. *Trends Mol Med* 2007;13:363–72.
11. Chi P, Allis CD, Wang GG. Covalent histone modifications—miswritten, misinterpreted and mis-erased in human cancers. *Nat Rev Cancer* 2010;10:457–69.
12. Ayton PM, Cleary ML. Molecular mechanisms of leukemogenesis mediated by MLL fusion proteins. *Oncogene* 2001;20:5695–707.
13. Krivtsov AV, Armstrong SA. MLL translocations, histone modifications and leukaemia stem-cell development. *Nat Rev Cancer* 2007;7:823–33.
14. Reader JC, Meekins JS, Gojo I, Ning Y. A novel NUP98-PHF23 fusion resulting from a cryptic translocation t(11;17)(p15;p13) in acute myeloid leukemia. *Leukemia* 2007;21:842–4.
15. Wang GG, Song J, Wang Z, Dormann HL, Casadio F, Li H, et al. Hematopoietic malignancies caused by dysregulation of a chromatin-binding PHD finger. *Nature* 2009;459:847–51.
16. Chung YJ, Choi CW, Slape C, Fry T, Aplan PD. Transplantation of a myelodysplastic syndrome by a long-term repopulating hematopoietic cell. *Proc Natl Acad Sci U S A* 2008;105:14088–93.
17. Caudell D, Zhang Z, Chung YJ, Aplan PD. Expression of a CALM-AF10 fusion gene leads to Hoxa cluster overexpression and acute leukemia in transgenic mice. *Cancer Res* 2007;67:8022–31.
18. Deshpande AJ, Cusan M, Rawat VP, Reuter H, Krause A, Pott C, et al. Acute myeloid leukemia is propagated by a leukemic stem cell with lymphoid characteristics in a mouse model of CALM/AF10-positive leukemia. *Cancer Cell* 2006;10:363–74.
19. Morse HC III, Anver MR, Fredrickson TN, Haines DC, Harris AW, Harris NL, et al. Bethesda proposals for classification of lymphoid neoplasms in mice. *Blood* 2002;100:246–58.
20. Ashworth TD, Pear WS, Chiang MY, Blacklow SC, Mastio J, Xu L, et al. Deletion-based mechanisms of Notch1 activation in T-ALL: key roles for RAG recombinase and a conserved internal translational start site in Notch1. *Blood* 2010;116:5455–64.
21. Ivanova NB, Dimos JT, Schaniel C, Hackney JA, Moore KA, Lemischka IR. A stem cell molecular signature. *Science* 2002;298:601–4.
22. Valk PJ, Verhaak RG, Beijnen MA, Erpelinck CA, Barjesteh van Doorn-Khosrovani S, Boer JM, et al. Prognostically useful gene-expression profiles in acute myeloid leukemia. *N Engl J Med* 2004;350:1617–28.
23. Zhang J, Ding L, Holmfeldt L, Wu G, Heatley SL, Payne-Turner D, et al. The genetic basis of early T-cell precursor acute lymphoblastic leukaemia. *Nature* 2012;481:157–63.
24. Chervinsky DS, Lam DH, Zhao XF, Melman MP, Aplan PD. Development and characterization of T cell leukemia cell lines established from SCL/LMO1 double transgenic mice. *Leukemia* 2001;15:141–7.
25. Wagner EK, Nath N, Flemming R, Feltenberger JB, Denu JM. Identification and characterization of small molecule inhibitors of a plant homeodomain finger. *Biochemistry* 2012;51:8293–306.
26. Gough SM, Chung YJ, Aplan PD. Depletion of cytotoxic T-cells does not protect NUP98-HOXD13 mice from myelodysplastic syndrome but reveals a modest tumor immunosurveillance effect. *PLoS ONE* 2012;7:e36876.
27. Matutes E, Morilla R, Farahat N, Carbonell F, Swansbury J, Dyer M, et al. Definition of acute biphenotypic leukemia. *Haematologica* 1997;82:64–6.
28. Chervinsky DS, Zhao XF, Lam DH, Ellsworth M, Gross KW, Aplan PD. Disordered T-cell development and T-cell malignancies in SCL LMO1 double-transgenic mice: parallels with E2A-deficient mice. *Mol Cell Biol* 1999;19:5025–35.
29. Lin YW, Nichols RA, Letterio JJ, Aplan PD. Notch1 mutations are important for leukemic transformation in murine models of precursor-T leukemia/lymphoma. *Blood* 2006;107:2540–3.
30. Swerdlow SH, Campo E, Harris NL, Jaffe ES, Pileri SA, Stein H, et al. editors. WHO classification of tumors of haematopoietic and lymphoid tissues. Lyon, France: IARC Press; 2008.
31. Weng AP, Ferrando AA, Lee W, Morris J IV, Silverman LB, Sanchez-Irizarry C, et al. Activating mutations of NOTCH1 in human T cell acute lymphoblastic leukemia. *Science* 2004;306:269–71.
32. Sauvageau G, Lansdorp PM, Eaves CJ, Hogge DE, Dragowska WH, Reid DS, et al. Differential expression of homeobox genes in functionally distinct CD34<sup>+</sup> subpopulations of human bone marrow cells. *Proc Natl Acad Sci U S A* 1994;91:12223–7.
33. Huang Y, Sitwala K, Bronstein J, Sanders D, Dandekar M, Collins C, et al. Identification and characterization of Hoxa9 binding sites in hematopoietic cells. *Blood* 2012;119:388–98.
34. Schuringa JJ, Chung KY, Morrone G, Moore MA. Constitutive activation of STAT5A promotes human hematopoietic stem cell self-renewal and erythroid differentiation. *J Exp Med* 2004;200:623–35.
35. Homminga I, Pieters R, Meijerink JP. NKL homeobox genes in leukemia. *Leukemia* 2012;26:572–81.
36. Pabst O, Zweigerdt R, Arnold HH. Targeted disruption of the homeobox transcription factor Nkx2-3 in mice results in postnatal lethality and abnormal development of small intestine and spleen. *Development* 1999;126:2215–25.
37. Siddique HR, Saleem M. Role of BMI1, a stem cell factor, in cancer recurrence and chemoresistance: preclinical and clinical evidences. *Stem Cells* 2012;30:372–8.
38. Buitenkamp TD, Pieters R, Gallimore NE, van der Veer A, Meijerink JP, Beverloo HB, et al. Outcome in children with Down's syndrome and acute lymphoblastic leukemia: role of IKZF1 deletions and CRLF2 aberrations. *Leukemia* 2012;26:2204–11.
39. Lee MS, Hanspers K, Barker CS, Korn AP, McCune JM. Gene expression profiles during human CD4<sup>+</sup> T cell differentiation. *Int Immunopharmacol* 2004;16:1109–24.
40. Bureau C, Hanoun N, Torrisani J, Vinel JP, Buscail L, Cordelier P. Expression and function of Kruppel like-factors (KLF) in carcinogenesis. *Curr Genomics* 2009;10:353–60.
41. Deshpande AJ, Bradner J, Armstrong SA. Chromatin modifications as therapeutic targets in MLL-rearranged leukemia. *Trends Immunol* 2012;33:563–70.
42. Bernstein BE, Mikkelsen TS, Xie X, Kamal M, Huebert DJ, Cuff J, et al. A bivalent chromatin structure marks key developmental genes in embryonic stem cells. *Cell* 2006;125:315–26.
43. Yang N, Xu RM. Structure and function of the BAH domain in chromatin biology. *Crit Rev Biochem Mol Biol* 2013;48:211–21.
44. Cvek B. Targeting malignancies with disulfiram (Antabuse): multi-drug resistance, angiogenesis, and proteasome. *Curr Cancer Drug Targets* 2011;11:332–7.
45. Malcolm MT. Disulfiram blood levels. *Br Med J* 1977;2:457.
46. Kasper LH, Brindley PK, Schnabel CA, Pritchard CE, Cleary ML, van Deursen JM. CREB binding protein interacts with nucleoporin-specific FG repeats that activate transcription and mediate NUP98-HOXA9 oncogenicity. *Mol Cell Biol* 1999;19:764–76.
47. Ogilvy S, Metcalf D, Gibson L, Bath ML, Harris AW, Adams JM. Promoter elements of vav drive transgene expression in vivo throughout the hematopoietic compartment. *Blood* 1999;94:1855–63.
48. Schlissel MS, Corcoran LM, Baltimore D. Virus-transformed pre-B cells show ordered activation but not inactivation of immunoglobulin gene rearrangement and transcription. *J Exp Med* 1991;173:711–20.
49. Beachy SH, Onozawa M, Chung YJ, Slape C, Bilke S, Francis P, et al. Enforced expression of Lin28b leads to impaired T-cell development, release of inflammatory cytokines, and peripheral T-cell lymphoma. *Blood* 2012;120:1048–59.
50. Slape C, Chung YJ, Soloway PD, Tessarollo L, Aplan PD. Mouse embryonic stem cells that express a NUP98-HOXD13 fusion protein are impaired in their ability to differentiate and can be complemented by BCR-ABL. *Leukemia* 2007;21:1239–48.

# CANCER DISCOVERY

## NUP98–PHF23 Is a Chromatin-Modifying Oncoprotein That Causes a Wide Array of Leukemias Sensitive to Inhibition of PHD Histone Reader Function

Sheryl M. Gough, Fan Lee, Fan Yang, et al.

*Cancer Discovery* 2014;4:564–577. Published OnlineFirst February 17, 2014.

**Updated version** Access the most recent version of this article at:  
[doi:10.1158/2159-8290.CD-13-0419](https://doi.org/10.1158/2159-8290.CD-13-0419)

**Supplementary Material** Access the most recent supplemental material at:  
<http://cancerdiscovery.aacrjournals.org/content/suppl/2014/02/17/2159-8290.CD-13-0419.DC1.html>

**Cited articles** This article cites 49 articles, 25 of which you can access for free at:  
<http://cancerdiscovery.aacrjournals.org/content/4/5/564.full.html#ref-list-1>

**Citing articles** This article has been cited by 2 HighWire-hosted articles. Access the articles at:  
[/content/4/5/564.full.html#related-urls](http://cancerdiscovery.aacrjournals.org/content/4/5/564.full.html#related-urls)

**E-mail alerts** [Sign up to receive free email-alerts](#) related to this article or journal.

**Reprints and Subscriptions** To order reprints of this article or to subscribe to the journal, contact the AACR Publications Department at [pubs@aacr.org](mailto:pubs@aacr.org).

**Permissions** To request permission to re-use all or part of this article, contact the AACR Publications Department at [permissions@aacr.org](mailto:permissions@aacr.org).